

Equivalent background speed in recovery from motion adaptation

William A. Simpson, Aaron Newman, and Wendi Aasland

Department of Psychology, University of Winnipeg, 515 Portage Avenue, Winnipeg, Manitoba, Canada R3B 2E9

Received April 8, 1996; revised manuscript received July 31, 1996; accepted August 7, 1996

We measured, in the same observers, (1) the detectability, d , of a small rotational jump following adaptation to rotational motion and (2) the detectability of the same jump when superimposed on one of several background rotation speeds. Following 90 s of motion adaptation the detectability of the jump was impaired, and sensitivity slowly recovered over the course of 60 s. The detectability of the jump was also impaired by the background speed in a way consistent with a quadratic form of Weber's law. We propose that motion adaptation impairs the detectability of the small jump because it is as if an equivalent background speed has been superimposed on the display. We measured the equivalent background by finding the real background speed that produced the same d' at each instant in the recovery from motion adaptation. The equivalent background started at approximately one to two thirds the speed of the adapting motion, declined rapidly, rose to a small peak at 30 s, then disappeared by 60 s. Since the equivalent background speed corresponds to the speed of the motion aftereffect, we have measured the time course of the motion aftereffect with objective psychophysics. © 1997 Optical Society of America. [S0740-3232(97)02601-X]

1. INTRODUCTION

After adaptation to a moving pattern the perceived motion of subsequently viewed patterns is altered.¹⁻³ We will show that motion adaptation reduces the detectability of a small jump (motion impulse⁴). Detectability is most impaired immediately after the end of the adaptation phase, and it gradually recovers over time. We propose that the motion detection impairment is due to an equivalent background⁵⁻⁹ speed that is superimposed, in the visual system, on the representation of the actual stimulus. Thus the effective task is one of speed increment detection. In a companion experiment we measure the impairment in jump detectability caused by a real background speed. The two experiments in combination allow us to measure the equivalent background in the motion system produced by adaptation. This equivalent background corresponds to the speed of the motion aftereffect. Thus, for the first time, we measure the motion aftereffect with objective psychophysics.

We now develop the predictions for the speed increment detection experiment and the recovery from motion adaptation experiment.

A. Speed Increment Detection

In a speed increment experiment the observer first adapts to an ongoing background rotational speed v , which is continuously present throughout the experiment. Then, in signaled intervals, an impulsive speed increment of size Δv may be added to the background speed. The size of the increment Δv is fixed, and the background speed v is varied. The speed waveform $v(t)$ for the speed increment stimulus can be expressed symbolically as

$$v(t) = v + \Delta v \delta(t - T), \quad (1)$$

where $\delta(t - T)$ is a Dirac delta function¹⁰ occurring at time T . In the luminance version of this experiment the

observer adapts to some background luminance upon which incremental flashes are superimposed.¹¹ We have done a thorough search, including the old literature surveyed by Brown,¹² and have failed to find a speed increment detection experiment. The existing studies of speed discrimination either have used a difference discrimination paradigm or have presented a speed step. In both of these classes of experiment there is no continuously viewed background speed; instead, discrete trials are presented, with a blank display between trials. In difference discrimination a single speed, v or $v + \Delta v$, is seen on each trial.¹³ In the speed step experiment the speed abruptly steps from v to $v + \Delta v$ or $v - \Delta v$ and stays there.¹⁴⁻¹⁶ The speed waveform for the speed step stimulus is

$$v(t) = v + \Delta v u(t - T), \quad (2)$$

where $u(t - T)$ is the Heaviside or unit step function.¹⁰

We now develop a signal detection model for the detectability of the impulsive speed increment. In the absence of some form of internal noise the increment will be perfectly detectable. Therefore we propose that normal (Gaussian) motion noise with mean n and variance σ^2 be superimposed on the stimulus representation.^{17,18} To keep the model simple, we ignore the fact that the speed increment is an impulse embedded in an extended stochastic process. On signal trials the observer has $v + \Delta v + N(n, \sigma^2) = N(v + \Delta v + n, \sigma^2)$; on noise trials the observer has $v + N(n, \sigma^2) = N(v + n, \sigma^2)$. The detectability d' is defined as the difference of the means of the two normal random variables divided by their standard deviation:

$$d' = \frac{(v + \Delta v + n) - (v + n)}{\sigma} = \frac{\Delta v}{\sigma}. \quad (3)$$

This simple signal detection model predicts that the detectability of the impulsive increment should not depend

at all on the speed of the background. There are no speed increment data available to test this prediction, though the data from speed step experiments are not consistent with it. The threshold Δv_{thresh} for detecting the presence of the speed step was measured and found to rise with the background speed. The data are replotted in Fig. 1. In Weber's law the step threshold Δv_{thresh} rises linearly with the background speed:

$$\Delta v_{\text{thresh}} = \sigma_0 + k v. \quad (4)$$

The above formulation of Weber's law includes a term for the absolute or detection speed threshold σ_0 , and k is the Weber fraction. The plotted data are not well fit by a line. The data require an added quadratic term in the model, as the U-shaped pattern in the residual plot makes clear (middle row of Fig. 1). Weber's law with quadratic term,

$$\Delta v_{\text{thresh}} = \sigma_0 + k_1 v + k_2 v^2, \quad (5)$$

describes the data well. The sizes of the fitted quadratic term with a 95% confidence interval are as follows: Hick, 0.007 ± 0.002 ; Notterman and Page, 0.0036 ± 0.0009 ; and De Bruyn and Orban, 0.0009 ± 0.0002 .

Let us assume that the impulsive speed increment threshold for rotational motion follows the same pattern as that seen for the step threshold for linear motion. In our experiment the observer views a pattern that rotates counterclockwise continuously except when a superimposed impulsive increment Δv occurs. We expect a form

of masking. (Masking: detectability of a fixed increment declines as the background increases; Weber's law: increment threshold rises as background increases.) The equation for masking corresponding to the quadratic near miss of Weber's law is

$$d' = \frac{\Delta v}{\sigma_0 + k_1 v + k_2 v^2}, \quad (6)$$

which the reader can confirm by setting d' to its value at threshold, 1, and solving for Δv . A comparison of Eqs. (3) and (6) shows that masking is produced when the standard deviation of the internal noise (the denominator of both equations) is proportional to the background speed.

B. Equivalent Background

Every 2 s in the time course of recovery from motion adaptation we measured the detectability of the same fixed size jump Δv as that used in the increment detection experiment. The equivalent background idea asserts that the detectability of the jump at each instant, $d'(t)$, is impaired by motion adaptation because the adaptation has produced an internal equivalent background speed $v_{\text{eq}}(t)$. Substituting $v_{\text{eq}}(t)$ for v in Eq. (6), we obtain

$$d'(t) = \frac{\Delta v}{\sigma_0 + k_1 v_{\text{eq}}(t) + k_2 v_{\text{eq}}^2(t)}. \quad (7)$$

We can now solve for $v_{\text{eq}}(t)$:

$$v_{\text{eq}}(t) = \frac{\sqrt{[d'(t)]^2 k_1^2 - 4[d'(t)]^2 k_2 \sigma_0 + 4d'(t) k_2 \Delta v - d'(t) k_1}}{2d'(t) k_2}. \quad (8)$$

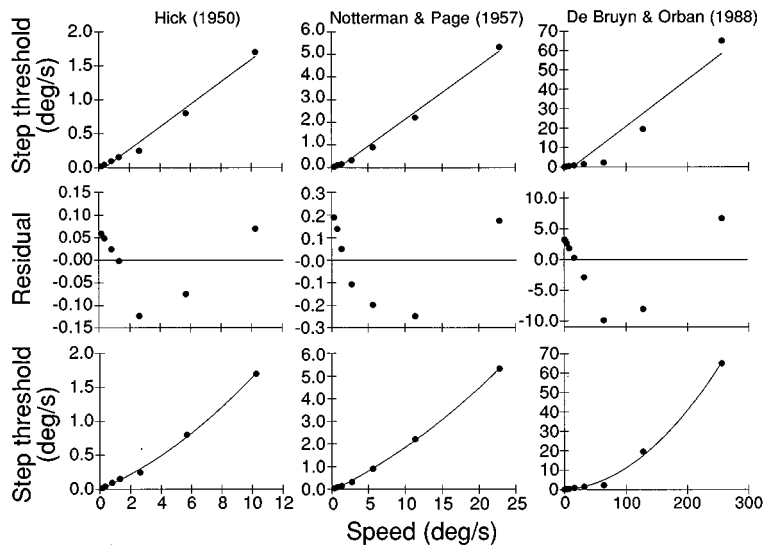


Fig. 1. Thresholds for detecting a speed step of linear motion. From left to right are replotted data from Hick,¹⁵ Notterman and Page,¹⁶ and De Bruyn and Orban.¹⁴ For the Hick data the average of the step increments and decrements is plotted. The De Bruyn and Orban data are for random dots. The top row shows the fit of Weber's law, Eq. (4). The middle row shows the residuals. The U-shaped pattern in the residuals shows that one needs a quadratic component to fit the data. The bottom row shows the fit of Weber's law with quadratic component, Eq. (5). Note the different scales on the plots.

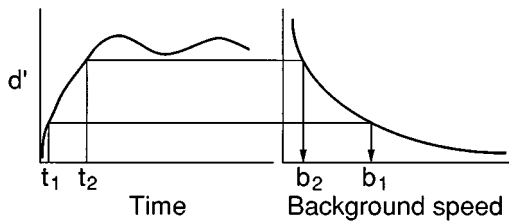


Fig. 2. The equivalent background computation is shown graphically. The same observer has produced results for the motion adaptation and increment detection experiments. The detectability, d' , of a small motion jump is plotted as a function of time after adaptation and as a function of the background speed upon which it is superimposed. The equivalent background speed is the background speed producing the same d' at any given point in the recovery from adaptation time course. The equivalent background at t_1 is b_1 and at t_2 is b_2 .

Equation (8) is the means by which we can measure the equivalent background at each instant in the recovery from motion adaptation. Figure 2 shows graphically how the equivalent background is computed.

In the motion adaptation experiment the adapting motion is clockwise, and the jump to be detected is counterclockwise. After rotating continuously for 90 s, the adapting pattern stops (except for the intermittent jumps to be detected). The motion aftereffect is counterclockwise. Thus the jump is in the same direction as that of the motion aftereffect. In the speed increment detection experiment we measured the detectability of a counterclockwise jump against a counterclockwise background speed. Together, we have a counterclockwise increment on a counterclockwise background that is real or adaptation induced (equivalent background). By finding the real background speed in the increment detection experiment that produces the same value of d' at each instant in the motion adaptation recovery time course, we measure the equivalent background. The equivalent background corresponds to the speed of the motion aftereffect.

2. METHODS

A. Observers

Two of the authors, WA and AN, served as observers. Both are well-corrected myopes, experienced in motion psychophysics.

B. Apparatus

The displays were generated by an MS-DOS computer connected to a point-plotting memory buffer developed at the University of Alberta¹⁹ and manufactured by Interactive Electronic Systems (Edmonton, Alberta, Canada). The plotter displayed the stimuli on a Tektronix 608 oscilloscope with P15 phosphor. The moving displays were viewed in a dark room with no veiling luminance. If we had used an oscilloscope with P31 phosphor, a veiling luminance would have been necessary to obscure the highly visible lingering phosphor trails.²⁰ The system can plot a dot having roughly a diameter of 2.6 min (at 1-m viewing distance) anywhere on a 4096×4096 grid. One dot is plotted per microsecond. The displays used 2000 dots, so a frame was refreshed at a rate of 500 Hz. Viewing was

monocular from a chin-and-forehead rest. At the 1-m viewing distance the total display area was 4×4 deg vertically and horizontally. Responses were collected by the computer by means of a button box.

C. Stimuli

1. Increment Detection

The stimulus was a set of rotating spokes. We measured the observer's ability to detect a small rotational displacement increment of fixed size (0.34 deg counterclockwise) at each of several background speeds. There was a real background counterclockwise rotation, and the rotational increment was in the same direction (see Fig. 3). In the partner recovery from motion adaptation experiment the background counterclockwise rotation was illusory, created by adaptation to clockwise rotation. The test jump to be detected in this experiment was thus in the same counterclockwise direction as that of the motion aftereffect.

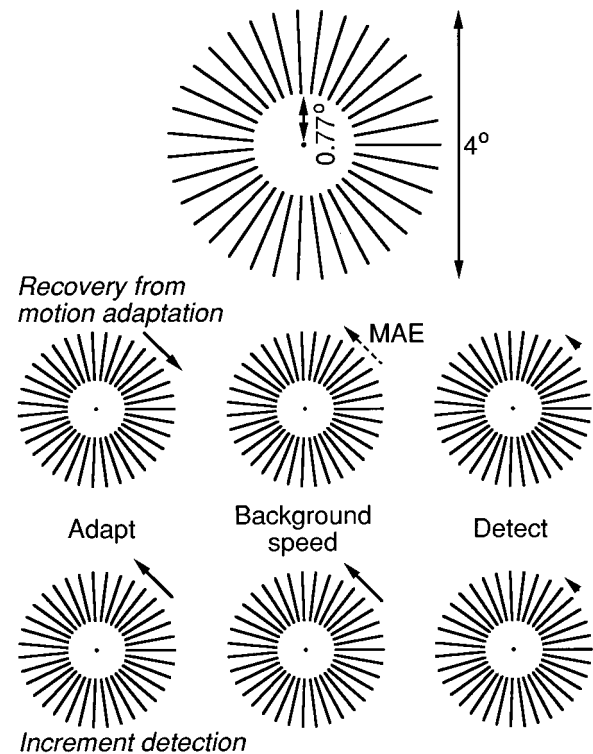


Fig. 3. The top row shows a scale diagram of the pattern used. The diagram is reversed contrast: In the experiments the lines were bright on a dark background. The middle row shows the plan of the recovery from motion adaptation experiment. The observer adapted to a clockwise rotating pattern for 90 s. Then it stopped rotating, and the observer experienced the counterclockwise equivalent background or motion aftereffect (MAE) shown. Periodically, a small counterclockwise impulsive rotation was presented for detection. The bottom row shows the plan of the increment detection experiment. The observer adapted to 90 s of counterclockwise rotation. The pattern continued rotating at this same background speed throughout the experiment. Periodically, an impulsive rotation increment was added to the background speed for detection.

The stimulus was a set of spokes in a rimless wheel (see Fig. 3). The spokes rotated continuously at 0, 3.4, 6.8, 10.3, 13.7, 17.1, or 20.6 deg s⁻¹. The direction of the rotation was counterclockwise. Every 3 s a click signaled a trial period during which a small counterclockwise jump (0.34 deg) could have occurred (with a probability near 50%).

At the center of the wheel was a fixation mark made up of five superimposed dots. The display was blank around the fixation mark. The radius of the dark hub was 0.77 deg. Outside the hub were 35 spokes, evenly spaced around the wheel. Each spoke was constructed from 57 dots whose centers were spaced 1.3 min apart. At this spacing the dots joined into a solid line. Each spoke was a dot wide, approximately 2.6 min. The spokes stretched from an eccentricity of 0.77 deg to 2 deg.

The luminance as measured by a Minolta LS-100 photometer was 0.040 cd m⁻² for the background, 408.4 cd m⁻² for the fixation point, and 79.5 cd m⁻² for the dots in the spokes. The luminance was measured as follows. For the background the stimulus was displayed on the screen, and the photometer was aimed at a blank area on the screen away from where the stimulus was plotted. For the fixation point a 20 × 20-dot array was plotted with a separation of 1.3 min. Each dot was plotted five times (since the fixation mark was plotted five times in the experiment), so the array was made up of a total of 2000 dots. To determine the luminance of the spokes, we plotted another array of 44 × 44 dots with the same interdot separation. Each dot in this case was only plotted once. To bring the total number of dots up to 2000, we plotted 64 extra dots in one corner of the display far from the matrix.

We found it convenient to use polar coordinates in constructing the display. In polar coordinates rotation is performed simply by the incrementing of θ . A spoke is just a set of points with the same θ but increasing r . The polar coordinates were converted to Cartesian coordinates before plotting by the relations $x = r \cos \theta$ and $y = r \sin \theta$.

The motion was generated with a sequence of frames. Each frame, as described above, was composed of 2000 dots and so was refreshed at 500 Hz. Each frame in the motion sequence was displayed for 50 ms (in other words, the frame was repeated 25 times). Sixty frames were constructed. In each successive frame every spoke was rotated 0.17 deg counterclockwise relative to its position in the previous frame. In the actual running of the experiment not all of these generated frames were necessarily used. If every frame was displayed, then a 0.17-deg/frame rotation resulted. If every other frame was displayed, then the rotation was 0.34 deg/frame. By varying the number of skipped frames, one could generate a range of background speeds. So we varied the background speed by altering the rotational displacement and keeping the frame rate fixed. It is known that rotational motion of a display like ours can result in apparent backward motion for certain combinations of frame duration and rotational displacement.²¹ Such aliasing was not observed in our displays with the frame rate and rotational displacements that we used.

The method of generating the background speed has

just been described. The increment was created as follows. The increment was fixed at 0.34 deg. This corresponds to two frames of displacement in the 60-frame sequence. So after one complete revolution of the wheel, the next cycle skipped two frames. For example, if the slowest background speed was used, then all frames from 0 to 59 were displayed. After frame 59 the next frame to be displayed would be frame 0 if no increment were presented. With an increment the frame after frame 59 would be frame 2.

2. Time Course of Recovery from Motion Adaptation

The wheel described in Subsection 2.C.1 rotated clockwise during the adaptation phase. During the recovery phase the wheel was mostly stationary. Every 2 s a beep signaled a trial period during which a small counterclockwise jump (0.34 deg) could have occurred (with a probability near 50%). In the adaptation phase of the experiment the wheel rotated in apparent motion. The method of creating the motion was the same as that used in the increment detection experiment. In each successive frame the wheel was rotated clockwise relative to its position in the previous frame by 1.53 deg. Since the frame duration was 50 ms, the average speed of rotation was 30.8 deg s⁻¹.

D. Procedure

1. Increment Detection

We aimed to make the procedures of the two experiments—increment detection and motion adaptation—as similar as possible (see the bottom row of Fig. 3). Both experiments used an initial 90-s adaptation period. In the increment detection task the direction of rotation was counterclockwise. After the initial adaptation the observer was presented with a series of trials, each signaled by a click, that either contained a counterclockwise speed increment (jump) or did not. Exactly equal numbers of the two types of stimulus were presented in random order. The trials were presented every 3 s. Note that the background speed was continuously presented.

Each experimental run consisted of 50 trials. The hits and the false alarms over the whole block were recorded. The different background speeds were run in random order, with the constraint that all speeds were run once before any was run twice, etc. Each d' was based on 200–250 trials, with the exception of the stationary background, which was based on 1550 trials. The stationary background had many trials because it was essentially the motion adaptation experiment done with an adaptation speed of zero. We ran this as a control. For increment detection the time aspect was not needed, so we averaged the 50 trials every 2 s for 60 s: $50 \times 31 = 1550$.

2. Time Course of Recovery from Motion Adaptation

The plan of the experiment is shown in the middle row of Fig. 3. Observers fixated the central dot for 90 s while the spokes rotated. At the end of the adaptation period a tone sounded; 212 ms later the first test period was presented. In this postadaptation phase of the experiment the previously rotating spokes were now always station-

ary except in a test period. In a test period, signaled by a tone, a rotational jump could occur with a probability near 50%. The subject indicated whether or not a jump had occurred by pressing one of two buttons. No feedback was given.

The test periods (trials) occurred every 2 s. This inter-trial interval was shorter than the 3-s interval used in the increment detection experiment. A shorter interval was used here so that a detailed picture of the time course could be obtained. Observers had a maximum of 2 s to give a response for each trial. If a response was not given in this time for any of the 31 trials, the entire block of trials would be terminated and no data collected. However, 2 s was ample time to respond, and it was never necessary to terminate a session. Motion detectability was sampled every 2 s for 1 min, giving 31 trials altogether. Fifteen of the 31 trials in each set contained a jump, in which the otherwise stationary display was rotated counterclockwise with the use of a rotational jump of 0.34 deg (i.e., two of the rotational units described in Subsection 2.C.1). For the 16 other trials the display remained stationary. The order of the test stimuli was random.

An experimental run consisted of a 90-s adaptation phase followed by 31 test stimuli presented over the course of 60 s. Both subjects completed 50 runs, so, at each of the 31 times sampled, 50 test stimuli were presented and 50 responses were recorded. In order to ensure no carryover effect of the adaptation, we separated runs by a minimum of 2 h (typically several hours or even days), and a subject did a maximum of four runs per day.

3. Computation of d'

At each sampled instant (every 2 s) in the course of recovery from motion adaptation we counted the number of hits (response was "moving" when the test stimulus really moved), the number of times the stimulus really moved, the number of false alarms (response was "moving" when the test stimulus actually was stationary), and the number of times the stimulus was really stationary. From these numbers the d' for detecting the jump could be calculated for each instant in the time course of the recovery from motion adaptation.

Here is an illustration of the method with an example comprised of only four test periods. Suppose that the stimuli presented were moving, moving, not moving, and moving; the responses were "moving," "not moving," "moving," and "moving." Then the number of hits is 1, 0, 0, and 1; the number of moving stimuli is 1, 1, 0, and 1; the number of false alarms is 0, 0, 1, and 0; and the number of stationary stimuli is 0, 0, 1, and 0. On the next run the stimuli are moving, moving, not moving, and not moving, with responses "moving," "not moving," "moving," and "not moving." Then we have hits 1, 0, 0, and 0; moving stimuli 1, 1, 0, and 0; false alarms 0, 0, 1, and 0; and stationary stimuli 0, 0, 1, and 1. We now form the totals over the two runs: hits 2, 0, 0, and 1; moving stimuli 2, 2, 0, and 1; false alarms 0, 0, 2, and 0; and stationary stimuli 0, 0, 2, and 1. The proportions of hits and false alarms at each time are thus known, with the hit proportions 2/2, 0/2, 0/0, and 1/1 and the false alarm proportions 0/0, 0/0, 2/2, and 0/1. The precision of these

sample proportions increases with the number of runs. Once we have the hit and false alarm proportions, the estimated detectability of the motion is

$$d' = Z[p(\text{hit})] - Z[p(\text{false alarm})], \quad (9)$$

where $Z(\)$ denotes the inverse normal integral.

This experiment was taxing for subjects and took a long time to run, so we stopped collecting data after 50 runs. Unfortunately, 50 runs is rather small for estimating d' . One major problem with estimating d' with small numbers of trials is that sample hit proportions of 1 or false alarm proportions of 0 may result. The computation of d' requires finding the inverse normal integral of the proportions, and proportions of 1 and 0 give positive and negative infinities. Our solution was to form a three-point moving sum (like a three-point moving average but without dividing by 3) on the numbers of hits, moving stimuli, false alarms, and stationary stimuli. The new data points were defined as

$$\text{count}(i) = \text{count}(i - 1) + \text{count}(i) + \text{count}(i + 1), \quad (10)$$

where $\text{count}(i)$ is the number of the given sort of event at sampling time i ($i = 0$ to 30). The smoothed data points were thus based on 150, rather than on 50, stimuli. Bear in mind that this procedure is a sort of temporal low-pass filtering.²² We also present the unsmoothed hit and false alarm proportions.

Even after smoothing, in one case we had the problem of an obtained $p(\text{false alarm}) = 0$. The case in question was observer AN at the second-to-last test period; he had no false alarms in 69 presentations of the stationary stimulus. This is a problem, since the estimate of d' is infinite in this case. Our novel way of coping with this situation is explained in Appendix A.

3. RESULTS AND DISCUSSION

A. Increment Detection

The detectability of the speed increment as a function of the background speed is shown in Fig. 4. Weber's law for speed increment detection would give the function

$$d' = \frac{\Delta v}{\sigma_0 + kv}, \quad (11)$$

where Δv is the size of the speed increment, σ_0 is the absolute threshold, k is the Weber fraction, and v is the background speed. Although this function gave a good fit to WA's data, the fit to AN's data was poor (see below). Including a quadratic term in the denominator [Eq. (6)] resulted in good fits to both observers' data. Recall our discussion in Section 1 of the previous results for speed step detection¹⁴⁻¹⁶ that were well described by the corresponding threshold version of this equation, Eq. (5).

The obtained fits of Eq. (6) to the data in Fig. 4 were as follows. For WA the least-squares estimates with 95% confidence intervals are $\sigma_0 = 0.0973 \pm 0.004$, $k_1 = 0.0087 \pm 0.002$, and $k_2 = 0.00014 \pm 0.00016$. Note that for WA the 95% confidence interval for k_2 includes zero; since the quadratic term is not significantly different from zero, Eq. (11) fits these data. For AN the estimates with 95% confidence intervals are $\sigma_0 = 0.1072$

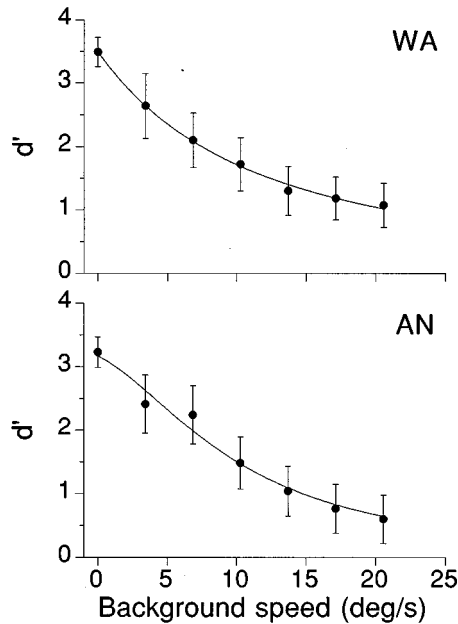


Fig. 4. Increment detection experiment for observers WA and AN. d' for the detection of an impulsive speed increment of fixed size (0.34 deg of rotation) is plotted as a function of the background speed. Error bars represent the 95% confidence intervals computed by the method of Gourevitch and Galanter.²³ The curves are least-squares fits of Eq. (6).

± 0.014 , $k_1 = 0.0037 \pm 0.0078$, and $k_2 = 0.0008$
 $k_2 = 0.0008 \pm 0.0007$. Even for AN the quadratic term is small, though omitting it results in a decided lack of fit at higher background speeds.

The increment detection data are consistent with the simple model given in Section 1: Internal normal noise is added to the stimulus speed, and if the resulting random variable is greater than a criterion, the observer responds, "Increment present." The standard deviation of the normal noise is a second-order polynomial, positively accelerated function of the background speed. It is the denominator of Eq. (6).

Why the internal noise variance should increase as the background speed increases is an unsolved problem. No completely satisfactory solution has been proposed in any domain in which Weber's law has been found. Note that we find a near miss of Weber's law, since we find it necessary to include a quadratic term. We do not have an explanation for the near miss.

Our speed increment detection data conform to the pattern previously observed for speed step detection. To explain this, one would have to examine carefully the precise nature of the speed waveform and its placement in the internal noise stochastic process, both of which we have ignored in the name of simplicity.

B. Recovery from Motion Adaptation

The detectability of the small rotational jump during recovery from motion adaptation is shown in Fig. 5. Early in the recovery period the jump is near threshold ($d' = 1$), but after 60 s the jump is highly detectable (d' near 3 or 3.5). Adaptation to 90 s of rotational motion

strongly impairs the detectability of the motion impulses, and this adaptation effect decays over the course of 1 min.

One interesting aspect of Fig. 5 is that the recovery from motion adaptation curve does not rise monotonically. Both observers show a clear dip in detectability near 30 s. The recovery from adaptation curve can be thought of as the step response of the motion system, and so a simple model to fit would be the step response of a low-pass filter:

$$d' = a[1 - \exp(-bt)], \quad (12)$$

where a represents the maximum response and b is the time constant. In Fig. 5 we fitted a combination of the low-pass filter response with normal (Gaussian) dips:

$$d'(t) = a[1 - \exp(-bt)] - c \exp\{-(t - d)/2e\}^2\} - f \exp\{-(t - g)/2h^2\}, \quad (13)$$

where c and f control the depth, d and g control the location, and e and h control the width of the first and second dips. If the recovery from adaptation curve were monotonically increasing, the fitted depth of the dips (c and f) would be zero. In fact, the fitted depth of each dip was significantly larger than zero. WA had dips ($\pm 95\%$ confidence interval) at 18.3 ± 1.2 s and 34.7 ± 1.3 s, with depths of $0.6d' \pm 0.4d'$ and $1.1d' \pm 0.2d'$, respectively. AN had dips at 30.8 ± 1.6 s and 51.6 ± 1.2 s, with depths of $0.8d' \pm 0.3d'$ and $0.7d' \pm 0.3d'$, respectively. Both observers had strong dips near 30 s after the end of adaptation and weaker ones either before or after the strong dip.

This oscillatory recovery from motion adaptation has also been found in a study²⁴ of single simple cells in cat area 17. In the nonstimulated condition Giaschi *et al.*

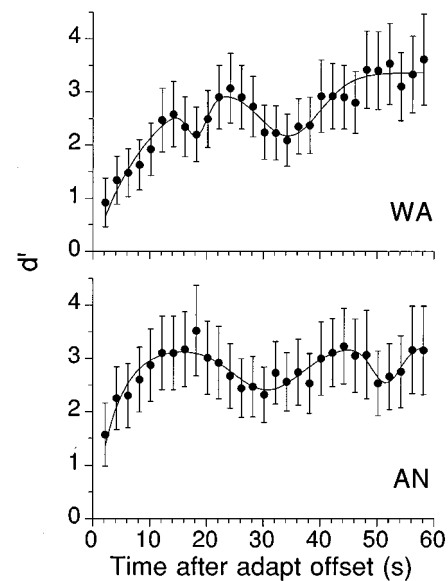


Fig. 5. Recovery from adaptation experiment for observers WA and AN. d' for the detection of impulsive rotation of fixed size (0.34 deg of rotation) is plotted as a function of the time elapsed from the offset of the adapting speed. Error bars represent the 95% confidence intervals computed by the method of Gourevitch and Galanter.²³ The curves are least-squares fits of Eq. (13).

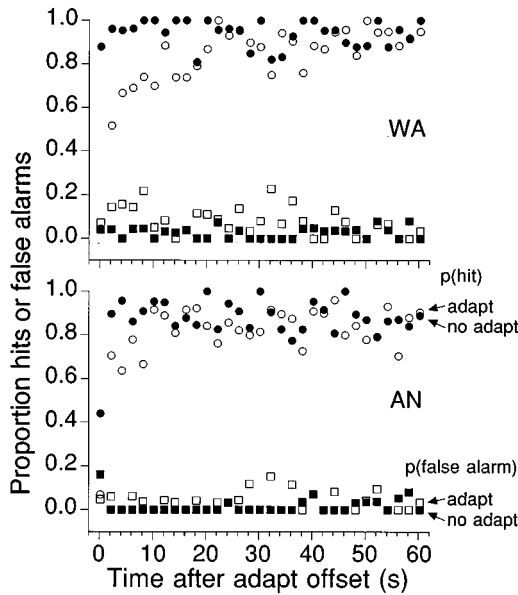


Fig. 6. Recovery from adaptation experiment for observers WA and AN. Unsmoothed proportions of hits and false alarms are plotted for adaptation to a stationary display (no adapt) and adaptation to 30.8-deg s^{-1} rotation (adapt).

adapted cells to their preferred direction of translational motion, then recorded their response to the opposite direction of motion. This is analogous to our motion adaptation condition, in which subjects adapted to counter-clockwise motion and then detected clockwise motion. The single cells show a clear oscillation with a dip in sensitivity near 50 s (see their Fig. 3B). Giaschi *et al.* used a longer adaptation time (120 s versus 90 s), and perhaps this accounts for the difference in the dip's location. Having pointed out concordant electrophysiological results, we hasten to stress that we used rotational motion, not translation. The simple cells that Giaschi *et al.* recorded from would not respond well to our stimulus (so they could not be the neural substrate).

The raw proportions of hits and false alarms over the time course of motion sensitivity recovery are shown in Fig. 6. Figure 5 is based upon a smoothed version of these data. The data patterns in Fig. 5 are also present in Fig. 6, indicating that the smoothing has not introduced artifacts. Figure 6 also shows the data from the control condition in which the adapting display was stationary. [Even smoothing would not allow d' to be calculated for these data, given the preponderance of $p(\text{hit}) = 1.0$ and $p(\text{false alarm}) = 0.0$.] Except for a low d' at the very start (especially for observer AN), the sensitivity of the observers is high throughout the recovery period. The low d' at the first trial is likely due to the observer's lack of readiness for the first test stimulus (which is understandable, given that he has just been staring at the adapting motion for 90 s).

C. Equivalent Background

The equivalent background is the background speed giving the same level of d' as that obtained at each moment in the course of recovery from motion adaptation. We

showed in Section 1 that the equivalent background speed is given by Eq. (8). The values of σ_0 , k_1 , and k_2 were obtained by least-squares fits of Eq. (6) to the increment detection data for each observer. Substituting these values into Eq. (8) gave the plots of the equivalent background time course in Fig. 7.

The equivalent background is high immediately after adaptation to the moving stimulus. At first, the equivalent background is approximately $10\text{--}23\text{ deg s}^{-1}$ counter-clockwise, which is approximately one to two thirds the speed of the adapting motion (30.8 deg s^{-1}) and opposite in direction to the adapting clockwise rotation. The equivalent background declines to zero by the end of 1 minute. Its intensity oscillates. As for the d' recovery from adaptation plot, each fitted curve in Fig. 7 is a combination of a low-pass filter step response and two normal peaks, although now the curve is reflected about the y axis:

$$v_{\text{eq}}(t) = a \exp(-bt) + c \exp\{-(t-d)/2e\}^2 + f \exp\{-(t-g)/2h\}^2. \quad (14)$$

Some authors²⁵ have proposed that the motion aftereffect speed declines exponentially over time. The equivalent background speed is a measure of the motion aftereffect speed. If the notion of exponential decay were correct, the confidence intervals for the heights of the fitted peaks would overlap with zero. In fact, the fitted height of each peak was significantly larger than zero. WA had peaks ($\pm 95\%$ confidence interval) at 18.4 ± 1.1 s and 34.4 ± 1.2 s, with heights of $3.8 \pm 2.0\text{ deg s}^{-1}$ and $5.8 \pm 1.1\text{ deg s}^{-1}$, respectively. AN had peaks at 30.5 ± 1.4 s and 51.6 ± 0.9 s, with heights of 4.5 ± 0.8

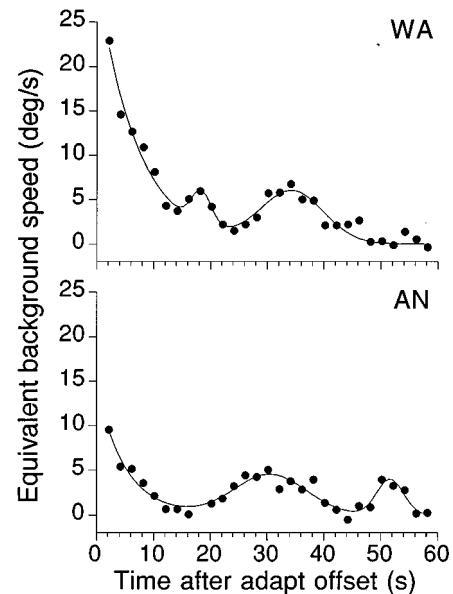


Fig. 7. Equivalent background speed at each moment in the time course of the recovery from motion adaptation experiment for observers WA and AN. Basically, it is the background speed in Fig. 4 yielding the same d' as that obtained in Fig. 5 at each moment (see the text for details). For reference, the adaptation speed was 30.8 deg s^{-1} . The curves are least-squares fits of Eq. (14).

deg s^{-1} and $4.0 \pm 1.4 \text{ deg s}^{-1}$, respectively. Both observers had strong peaks near 30 s after the end of adaptation and weaker ones either before or after the strong peak.

Anything that causes performance to decline will have the effect of raising the measured equivalent background. Thus one explanation of the peak in equivalent background at approximately 30 s is that it is due to a flagging of attention. The data from the control condition (Fig. 6) disprove this explanation. It can be seen that the cause of the decline of d' is primarily a rise in the false alarm rate, and this rise is absent in the stationary control condition.

In some studies the observer is instructed to hit a button²⁶ or report verbally²⁷ when the motion aftereffect has stopped, and this is used as a measure of the aftereffect duration. Figure 7 shows that this measure will be problematic, since the aftereffect stops and starts.

The plots of the equivalent background as a function of time after motion adaptation show the time course of the motion aftereffect, measured with objective psychophysics. Anstis has remarked that the motion aftereffect, "like piano music, is easy to record badly but hard to record well."²⁵ A good recording would use objective psychophysics, in which the subject is given a task that has an objectively correct answer on each trial.²⁸ Ours are the first objective psychophysical measurements of the motion aftereffect. Previous measurements of the time course of the rotational motion aftereffect have used magnitude estimation^{29,30} or nulling³¹ (others^{32,33} have used nulling but did not measure the time course).

A real background makes an increment hard to detect, we argue, because there is internal normal (Gaussian) speed noise whose standard deviation increases with the background [Eq. (6)]. Motion adaptation produces an apparent or equivalent background in the visual system that behaves in the same way as a real background [Eq. (7)]. In both cases the standard deviation of the noise rises as a function of the (real or equivalent) background. The equivalent background has the opposite direction to that of the adapting motion and corresponds to the speed of the motion aftereffect.

Subjective reports often describe the motion aftereffect as a paradoxical motion of a pattern that does not change position.²⁵ If the aftereffect does indeed consist of two parts, the equivalent background is a measure of the moving part.

4. CONCLUSIONS

We measured the detectability of a motion jump after adaptation to rotational motion. We also measured increment detection against various background speeds. By running both experiments on the same observers, we were able to determine the background speed at each moment in the recovery from motion adaptation that gave the same level of motion detectability. This is the equivalent background. We propose that adapting to motion makes subsequent motion detection difficult because such adaptation elevates the standard deviation of the internal speed noise. This motion noise is equivalent to that created by a real moving background. The motion

noise or the equivalent background has the direction opposite to that of the adapting motion and corresponds to the motion aftereffect. We have thus measured the time course of the motion aftereffect with objective psychophysics.

APPENDIX A: CALCULATING d' WHEN THE SAMPLE PROPORTION IS 0 OR 1

We now describe how we dealt with an observed sample proportion of 0. Our method applies equally to sample proportions of 1. If one makes no adjustments, the estimated d' in these cases is infinite.

An *ad hoc* procedure is commonly used to adjust observed false alarm rates of 0: Replace it with $0.5/n$, where n is the number of trials.³⁴ A $1/n$ rule is also used sometimes. The idea behind the adjustment is that although we observe a proportion of 0, this is only an estimate of the true proportion. The normal model of signal detection theory tells us that it is impossible truly to have a false alarm proportion of 0, so the observed proportion is 0 only because of the binomial sampling variability of

$$\frac{\text{number of false alarms}}{\text{number of stationary stimuli}}. \quad (\text{A1})$$

Note that expression (A1) is both the maximum-likelihood estimator and the minimum-variance unbiased estimator of the population false alarm proportion.³⁵

The fact that expression (A1) has a binomial distribution allows us to devise an approach for handling observed zeros in a way that is not completely *ad hoc*. We can calculate the exact confidence interval for the true proportion, given the confidence level and the number of trials. The idea is that we can replace the sample proportion with the exact upper $k\%$ confidence limit. We then can make the statement that the true proportion is somewhere between the upper confidence limit and 0, and a lower bound for d' can be calculated. That is, we can make an estimate of d' that is conservative—the higher the confidence level for the false alarm proportion, the smaller the d' estimate.

Many readers will be familiar with approximations to the exact confidence interval for a sample proportion. These approximations use the normal distribution, though the true sampling distribution for the sample proportion is binomial. The 95% confidence limit in the normal approximation is $p \pm 2(\text{SE})$, where p is the sample proportion and SE is the standard error, equal to $\sqrt{p(1-p)/n}$. Obviously, if $p = 0$ or $p = 1$, the SE is 0, and so the upper confidence limit is the same as p , according to this approximation. In the exact confidence limits we can compute an upper confidence limit some nonzero distance away from the sample proportion even for observed proportions of 0 and 1.

The exact confidence limits are derived straightforwardly. The general two-sided exact confidence intervals are discussed by Rothman³⁶; Mehta³⁷ derives the one-sided confidence limits in our special case in the following way. The response on each trial is a Bernoulli random variable with probability of false alarm π . Thus the chance of 0 false alarms in n Bernoulli trials is

$(1 - \pi)^n$. The $k\%$ upper confidence limit for π is the value of π that gives a p value of $1 - k/100$. We have

$$(1 - \pi)^n = 1 - k/100.$$

So the one-sided exact $k\%$ upper confidence limit for the true proportion whose lower limit is 0 is

$$\text{UCL} = 1 - \left(1 - \frac{k}{100}\right)^{1/n}. \quad (\text{A2})$$

AN had no false alarms in 69 trials. With the use of $n = 69$ trials and the confidence level set at 95%, the upper confidence limit for the true proportion is 0.0425. This value might be used to replace the observed proportion of 0. The resulting d' will be quite conservative (low). (Remember that if no adjustment at all is done to the observed proportion, d' will be infinite.)

We can calculate the confidence level k associated with the two *ad hoc* rules. For the $1/n$ rule we substitute $1/n$ for UCL in Eq. (A2); solving for $k/100$, we find

$$\frac{k}{100} = 1 - \left(\frac{n-1}{n}\right)^n. \quad (\text{A3})$$

The $1/n$ rule tells us to replace the sample proportion of 0/69 with 1/69. With $n = 69$ we obtain $k = 63.5\%$ for the $1/n$ rule. In other words, if we obtain a sample proportion of 0/69, replacing it with 1/69 amounts to using the upper 63.5% confidence limit for the true proportion.

For the $0.5/n$ rule we substitute $0.5/n$ for UCL in Eq. (A2); solving for $k/100$, we find

$$\frac{k}{100} = 1 - \left(\frac{2n-1}{2n}\right)^n. \quad (\text{A4})$$

Replacing an obtained 0/69 with 0.5/69 amounts to using the upper 39.4% confidence limit for the true proportion.

The confidence level corresponding to these *ad hoc* rules is fairly constant no matter what the number of trials. For example, with the $1/n$ rule, an n of 25, 75, or 225 corresponds to a confidence level of 64.0%, 63.4%, or 63.3%.

The question remaining is, What confidence level to use? The 95% confidence level is used commonly in many statistical problems, but this level, it seems to us, leads to d' estimates that are too low. With an n of 69, for example, we would replace our observed 0/69 with 3/69. The $0.5/n$ rule, corresponding to a confidence level of 39%, seems to lead to d' estimates that are too high. We settle on a confidence level of 65%, near the $1/n$ rule's 63%–64%. This rule leads to fairly conservative d' estimates.

The above approach can also be applied to the case in which $p = 1$. This will typically happen with hit rates. In this case one needs the lower confidence limit for the proportion:

$$\text{LCL} = \left(1 - \frac{k}{100}\right)^{1/n}. \quad (\text{A5})$$

ACKNOWLEDGMENTS

We thank William Feuer, University of Miami, and Cyrus Mehta, Harvard University, for their help on the exact confidence limits for an observed proportion of 0 or 1. We thank Mike Swanston and Debbie Giaschi for their helpful comments on the manuscript. This work was supported by a Natural Sciences and Engineering Research Council research grant.

Address correspondence to William A. Simpson, who may be reached by telephone at (204) 786-9151, by fax at (204) 786-1824, and at the e-mail address wsimpson@uwinnipeg.ca.

REFERENCES

1. S. Anstis, "Motion perception in the frontal plane," in *Handbook of Perception and Human Performance*, K. R. Boff, L. Kaufman, and J. P. Thomas, eds. (Wiley, Toronto, 1986), Vol. 1, pp. 16-1-16-27.
2. M. T. Swanston and N. J. Wade, "A peculiar optical phenomenon," *Perception* **23**, 1107-1110 (1994).
3. N. J. Wade, "A selective history of the study of visual motion aftereffects," *Perception* **23**, 1111-1134 (1994).
4. W. A. Simpson, "Temporal summation of visual motion," *Vision Res.* **34**, 2547-2559 (1994).
5. B. H. Crawford, "The change of visual sensitivity with time," *Proc. R. Soc. London Ser. B* **123**, 69-89 (1937).
6. B. H. Crawford, "Visual adaptation in relation to brief conditioning stimuli," *Proc. R. Soc. London Ser. B* **134**, 283-302 (1947).
7. C. B. Blakemore and W. A. H. Rushton, "Adaptation and increment threshold in a rod monochromat," *J. Physiol. (London)* **181**, 612-628 (1965).
8. C. B. Blakemore and W. A. H. Rushton, "The rod increment threshold during dark adaptation in normal and rod monochromat," *J. Physiol. (London)* **181**, 629-640 (1965).
9. W. A. H. Rushton, "The Ferrier lecture: visual adaptation," *Proc. R. Soc. London, Ser. B* **162**, 20-46 (1965).
10. W. M. Siebert, *Circuits, Signals, and Systems* (McGraw-Hill, Toronto, 1986), pp. 314-335.
11. M. Aguilar and W. S. Stiles, "Saturation of the rod mechanism of the retina at high levels of stimulation," *Opt. Acta* **1**, 59-65 (1954).
12. R. H. Brown, "Visual sensitivity to differences in velocity," *Psychol. Bull.* **58**, 89-103 (1961).
13. S. P. McKee, "A local mechanism for differential velocity detection," *Vision Res.* **21**, 491-500 (1981).
14. B. De Bruyn and G. A. Orban, "Human velocity and direction discrimination measured with random dot patterns," *Vision Res.* **28**, 1323-1335 (1988).
15. W. E. Hick, "The threshold for sudden changes in the velocity of a seen object," *Q. J. Exp. Psychol.* **2**, 33-41 (1950).
16. J. M. Notterman and D. E. Page, "Weber's law and the difference threshold for the velocity of a seen object," *Science* **126**, 652-653 (1957).
17. W. A. Simpson and B. A. Finsten, "Pedestal effect in visual motion discrimination," *J. Opt. Soc. Am. A* **12**, 2555-2563 (1995).
18. S. N. J. Watamaniuk, "Ideal observer for discrimination of the global direction of dynamic random-dot stimuli," *J. Opt. Soc. Am. A* **10**, 16-28 (1993).
19. G. Finley, "A high-speed point plotter for vision research," *Vision Res.* **25**, 1993-1997 (1985).
20. R. Groner, M. T. Groner, P. Müller, W. F. Bischof, and V. Di Lollo, "On the confounding effects of phosphor persistence in oscilloscopic displays," *Vision Res.* **33**, 913-917 (1993).
21. P. Werkhoven and J. J. Koenderink, "Reversed rotary motion perception," *J. Opt. Soc. Am. A* **8**, 1510-1516 (1991).
22. A. V. Oppenheim, A. S. Willsky, and I. T. Young, *Signals and Systems* (Prentice-Hall, Toronto, 1983), pp. 414-420.

23. V. Gourevitch and E. Galanter, "A significance test for one-parameter isosensitivity functions," *Psychometrika* **32**, 25–33 (1967).
24. D. Giaschi, R. Douglas, S. Marlin, and M. Cynader, "The time course of direction-selective adaptation in simple and complex cells in cat striate cortex," *J. Neurophysiol.* **70**, 2024–2034 (1993).
25. Ref. 1, p. 16–5.
26. C. Bonnet and V. Pouthas, "Apparent size and duration of a movement after-effect," *Q. J. Exp. Psychol.* **24**, 275–281 (1972).
27. P. Lavie and Z. Giora, "Spiral aftereffect durations following awakening from REM sleep and non-REM sleep," *Percept. Psychophys.* **14**, 19–20 (1973).
28. D. M. Green and J. A. Swets, *Signal Detection Theory and Psychophysics* (Peninsula, Los Altos, Calif., 1988), pp. 121–126.
29. M. Hershenson, "Linear and rotation motion aftereffects as a function of inspection duration," *Vision Res.* **33**, 1913–1919 (1993).
30. R. Sekuler and A. Pantle, "A model for after-effects of seen movement," *Vision Res.* **7**, 427–439 (1967).
31. M. M. Taylor, "Tracking the decay of the after-effect of seen rotary movement," *Percept. Mot. Skills* **16**, 119–129 (1963).
32. G. Johansson, "The velocity of the motion after-effect," *Acta Psychol.* **12**, 19–24 (1956).
33. V. Steiner, R. Blake, and D. Rose, "Interocular transfer of expansion, rotation, and translation motion aftereffects," *Perception* **23**, 1197–1202 (1994).
34. N. A. MacMillan and C. D. Creelman, *Detection Theory: A User's Guide* (Cambridge U. Press, New York, 1988), p. 357.
35. S. D. Silvey, *Statistical Inference* (Chapman and Hall, New York, 1975).
36. K. J. Rothman, *Modern Epidemiology* (Little, Brown, Toronto, 1986), Chap. 11, pp. 165–170.
37. C. Mehta, *StatXact-3 for Windows User Manual* (Cytel Software Corp., Cambridge, Mass., 1995), Eqs. 9.37 and 9.38, pp. 220–221.